

Experimental Generation and Characterization of Uniformly Filled Ellipsoidal Electron-Beam Distributions

P. Musumeci, J. T. Moody, R. J. England, J. B. Rosenzweig, and T. Tran

Department of Physics and Astronomy, University California Los Angeles, Los Angeles, California, 90095, USA

(Received 6 December 2007; published 16 June 2008)

For 40 years, uniformly filled ellipsoidal beam distributions have been studied theoretically, as they hold the promise of generating self-fields linear in the coordinate offset in all three directions. Recently, a scheme for producing such distributions, based on the strong longitudinal expansion of an initially very short beam under its own space-charge forces, has been proposed. In this Letter we present the experimental demonstration of this scheme, obtained by illuminating the cathode in a rf photogun with an ultrashort laser pulse (~ 35 fs rms) with an appropriate transverse profile. The resulting 4 MeV beam spatiotemporal (x, t) distribution is imaged using a rf deflecting cavity with 50 fs resolution. A temporal asymmetry in the ellipsoidal profile, due to image charge effects at the photocathode, is observed at higher charge operation. This distortion is also found to degrade the transverse beam quality.

DOI: [10.1103/PhysRevLett.100.244801](https://doi.org/10.1103/PhysRevLett.100.244801)

PACS numbers: 29.25.Bx, 29.27.Bd, 41.75.Ht, 41.85.Ct

State-of-the-art high brightness electron source designs are most commonly based on use of a high gradient rf photoinjector, with a properly longitudinally and radially shaped laser pulse to illuminate the cathode [1]. In these schemes, which rely on the emittance-compensation process [2,3], approximately uniformly filled, temporally flat, cylindrical distributions are usually assumed in order to minimize the space-charge induced emittance growth. Obtaining such laser pulse shapes introduces a high degree of complexity in the photocathode drive laser, which is a key, technologically challenging component of the system. Moreover, the “beer-can” beam distribution, as it is often referred to, presents large nonlinearities in the space-charge field profiles at the beam longitudinal head and tail. These nonlinearities eventually give rise to irreversible emittance growth—as opposed to the reversible emittance growth dealt with by compensation—leading to the formation of bifurcated phase space distributions, as well as beam spatial halos [4].

The ideal beam distribution, where such irreversible beam dynamics would be entirely and self-consistently avoided, requires that the space-charge fields in each Cartesian dimension have linear dependence on the bunch coordinates. Such a condition is achieved for uniformly filled ellipsoidal distributions [5].

Despite their advantages, these distributions have not been considered a practical possibility until recently. One possibility for obtaining the uniform ellipsoidal density distribution is to similarly shape the laser pulse illuminating the cathode [6]; however, this solution further increases the complexity of the laser system. Another attractive option takes advantage of the ultrafast rearrangement of the beam as it expands longitudinally under the influence of strong space-charge forces. Luiten *et al.* [7], reconsidering an idea proposed by Serafini [8], have shown that to obtain a final ellipsoidal distribution there is essentially no requirement on the initial laser pulse shape other than it be much shorter than the final bunch length after expansion.

On the other hand, formation of the ellipsoidal beam distribution is sensitive to the radial laser profile, with the ideal proposed profile having radial dependence $\sqrt{1 - (r/a)^2}$ for $r \leq a$ (half-circle distribution). This mode of operation, where the optimized distribution is obtained by dynamical evolution from an initial ultrashort beam, has been termed the *blowout* regime of photoinjector operation, to emphasize the strong longitudinal space-charge expansion.

In this Letter we present the results of an experimental test of the blowout regime, performed at the UCLA Pegasus Laboratory, where a short laser pulse (~ 35 fs) was used to illuminate a metallic (Mg) cathode inside a standard 2.856 GHz 1.6 cell SLAC/BNL/UCLA rf gun. Previous attempts to observe this new regime have relied on methods with inadequate resolution, in nonideal conditions [9]. Here we report direct measurement of the beam temporal profile and spatiotemporal distribution, obtained with the aid of an X-band deflecting cavity [10] located 1.5 m downstream of the cathode, with clear experimental evidence of the formation of uniformly filled ellipsoidal beam distributions from space-charge dominated expansion. Increasing the surface charge density at the cathode to a level where the longitudinal space-charge field becomes comparable with the rf accelerating field, we have also observed the ellipsoidal beam shape evolve into an asymmetric distribution having an elongated tail. The development of this beam tail is predicted well by particle dynamics simulations [11]; it is due to the decelerating effect of the beam’s image charge at the cathode. The transverse quality of the beam has been measured and found—as expected—strongly correlated to the linearity of the space-charge fields and thus to the symmetry of the ellipsoidal beam distribution.

A schematic of the Pegasus beam line is displayed in Fig. 1. The rf gun in these experiments is operated at a peak field of 80 MV/m to maximize rf and beam stability. The emittance-compensation solenoid is used to focus the beam

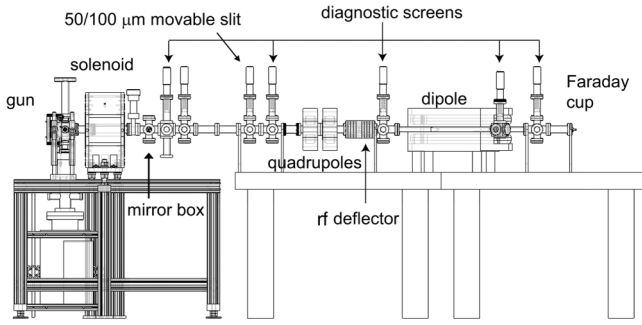


FIG. 1. Layout of Pegasus blowout regime experiment.

to a space-charge dominated waist a distance of 2.5 m from the cathode. A doublet of quadrupole lenses is employed to prepare the beam for the time-resolved measurements described below. A screen located after the 45° exit port of the dipole is used for energy measurements and a Faraday cup in the straight-through beam line allows determination of the beam charge.

A Ti:sapphire laser system from Coherent Inc. generates 40 fs FWHM at 800 nm as measured with a single shot autocorrelator. After frequency tripling in thin crystals (300 μm for second harmonic and 150 μm for third harmonic generation) and thin lens-based optical transport to the cathode the UV laser pulse is ~ 35 fs rms.

A $\nu = 9.599$ GHz 9-cell standing wave deflecting mode cavity [10] with a maximum deflecting voltage $V_0 = 500$ kV is used to impart a linear correlation between the temporal (t) position in the beam and the vertical position (y) detected on the downstream fluorescent screen. The proportionality factor between t and y on the screen located $L = 17$ cm from the cavity center is given by $K \simeq \frac{eV_0}{m_0c\gamma} \times \frac{2\pi\nu}{c} L \simeq 1.1$ fs/ μm , where c is the speed of light, e and m_0 are the electron charge and mass, and γ the Lorentz factor.

The low level reference signal at 9.599 GHz is obtained multiplying the 79.333 MHz laser oscillator master clock by 121. The rms jitter of the X-band signal with respect to the laser pulse introduced by this multiplication is ~ 1 ps. This results in a significant (~ 1 mm) vertical jitter of the beam position on the screen thus preventing collection of data by simple integration over multiple shots. For the measurements presented here a postprocessing routine selected data only from images for which the beam centroid was < 100 μm from the beam line axis.

The vertical rms beam size observed on the downstream screen can be approximately (exactly for Gaussian distributions) written as the quadrature sum of the contributions due to the deflection and the minimum rms spot size (σ_0) achieved when the cavity voltage is off, i.e., $\sigma_y \simeq \sqrt{\sigma_0^2 + (K\sigma_z/c)^2}$ where σ_z is the rms bunch length. In order to resolve the time structure of the bunch, we require that the contribution to the vertical spot size due to the t -correlated deflection largely exceeds σ_0 . The minimum measurable bunch length (which sets the temporal resolution) is given by σ_0/K .

Two different techniques were used to minimize σ_0 prior to turning on the deflecting voltage: (i) focusing with a quadrupole lens and (ii) selecting only the central beam “slice” by collimation using a horizontal slit. The information extracted from these different configurations is complementary, as in case (i) we measure the full beam distribution projected into 2D, while in case (ii) we measure only a nearly 2D slice extracted from it.

By employing the vertically focusing quadrupole just upstream of the rf cavity we focused the beam down to a thin ($\sigma_0 < 40$ μm thick) horizontal line on the measurement screen, yielding a temporal resolution better than 50 fs. The streak images obtained both before and after the 500 kV deflecting voltage is turned on, for the beam parameters given in Table I, are shown in Fig. 2.

Since the initial y -betatron size is negligible, there is an almost perfect correlation between the y axis and time. Thus one of the most striking features is the sharp ellipsoidal beam boundary which enclose the particle distribution function projected onto the (x, t) plane. The direct verification of this ellipsoidal boundary provides indeed a strong validation of the theoretical prediction of dynamical formation of ellipsoidal beams through ultrashort laser pulse cathode illumination.

The sharpness of the distribution boundary in t is predicted to be limited by the initial spread in emission times. The measured bunch length is 300 fs rms in good agreement with particle tracking simulations performed using the ASTRA beam dynamics code [12]. Even including the possible delay time associated with photoemission, the beam distribution has stretched by almost an order of magnitude. We then expect that it would show little memory of its initial size; the sharp density transition at the boundary verifies this expectation.

The intensity distribution inside the ellipse of Fig. 2(b) merits further consideration. Since the quadrupole lens focuses the beam in the vertical direction (y), effectively projecting the beam distribution along this axis, we expect an intensity distribution resembling the projection of a uniformly filled ellipsoid onto the x - z plane. In other words if the beam distribution $\rho(x, y, z)$ is constant and different than zero only for $\frac{x^2}{a^2} + \frac{y^2}{b^2} + \frac{z^2}{c^2} < 1$ where a, b, c are the three semiaxes of the ellipsoidal, on the screen one should observe an intensity distribution proportional to the projection of ρ onto the (x, z) plane $f(x, z) = \int \rho(x, y, z) dy \propto \sqrt{1 - \frac{x^2}{a^2} - \frac{z^2}{c^2}}$. This prediction is verified in Fig. 3, where a

TABLE I. Pegasus photoinjector parameters for the blowout regime

Beam energy	3.75 MeV
Peak field at the cathode	80 MV/m
Injection phase	25°
Beam charge	15 pC
Laser spot size (rms)	400 μm
Laser pulse length (rms)	35 fs

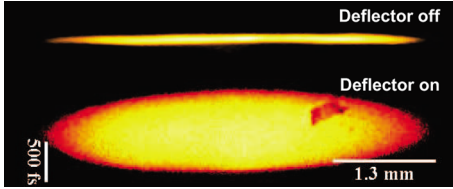


FIG. 2 (color online). Beam images after vertically focusing lens and rf deflector; cases with deflecting voltage off and on.

surface plot of the pixel intensities from Fig. 2(b) is compared to the ideal distribution $f(x, z)$.

Complementary information, where one directly samples a horizontal slice of the beam distribution, is obtained when a horizontal slit of $50 \mu\text{m}$ vertical aperture is inserted in the beam path. In this case the vertical beam size with the deflecting voltage turned off is $\sim 80 \mu\text{m}$, thus increasing the minimum temporal resolution by ~ 2 . A typical image for the beam parameters in Table I is shown in Fig. 4. The ellipsoidal beam boundary is evident also in this case. Moreover, plotting the pixel intensities along a line passing through the distribution center we obtain a flattop profile, as we would expect for the predicted uniformly filled ellipsoid.

In the original proposal of Ref. [7] the radial shape of the initial transverse laser profile is deemed critical for creating the ellipsoidal beam. However, in our measurements the initial laser transverse profile has been shaped by simply imaging onto the cathode an iris of aperture r_a illuminated with a larger Gaussian laser spot of measure σ_g . We observe in t -dependent beam images that the shape of the final beam distribution is not particularly sensitive to the initial transverse profile, as long as this one has sharp edges. Only when the laser transverse profile presents long tails, i.e., when the laser is apertured at a radius $r_a > 1.5\sigma_g$, does the beam lose its characteristic sharp ellipsoidal boundary. For the images given in Figs. 2–4, the cut was taken at $r_a = 0.8\sigma_g$ to improve the homogeneity of the emitted beam distribution.

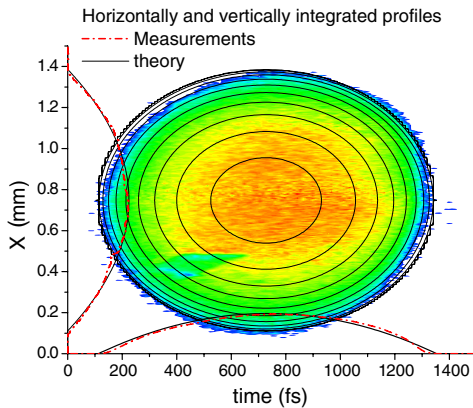


FIG. 3 (color online). Beam intensity distribution (color contour) from Fig. 2 and ideal uniformly filled ellipsoid (line contour) projected onto one axis.

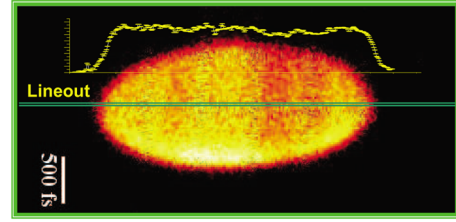


FIG. 4 (color online). Time-dependent image of beam with vertical collimation before deflector.

This mild dependence on the initial laser transverse shape is in good agreement with particle tracking simulations [13]. It originates in the details of the dynamics of the beam rearrangement. A half-circle initial distribution would be required if the beam expansion were entirely longitudinal. However, because of relativistic dilation the beam rest-frame aspect ratio—the ratio between the transverse and longitudinal beam sizes—grows very quickly to be of order unity. Hence the space-charge driven expansion and distribution rearrangement take place both radially and longitudinally, leading to an ellipsoidal boundary that is not critically dependent on the details of the initial conditions.

The streak image in Fig. 5 corresponds to a beam of charge $Q = 50 \text{ pC}$, and is taken in the projection (quadrupole-focused) mode. For this measurement, the phase of the deflecting field is such that an upward kick is imparted on the leading edge of the beam, which is thus found at the top of the image. For these charge levels, the beam after expansion is quite a bit longer ($>600 \text{ fs rms}$) and develops an asymmetry in the ellipsoidal boundary showing an elongated tail.

This effect is well predicted by simulations, as seen in the ASTRA phase space displayed in Fig. 5. It is due to the deceleration exerted on the beam in the near-cathode region by the beam image charge. This symmetry breaking in the longitudinal space-charge forces is always present, but becomes noticeable only when the magnitude of the image-induced electric field becomes a significant fraction of the rf accelerating field. In the case shown in Fig. 5, the surface charge density is 50 pC for a laser rms spot size at the cathode $\sigma_{L,\text{rms}} = 400 \mu\text{m}$. Including the image charge contribution, the peak decelerating field at the beam’s trailing edge is $E_{\text{SC,max}} = Q/[2\pi\sigma_{L,\text{rms}}^2\epsilon_0] = 5.6 \text{ MV/m}$,

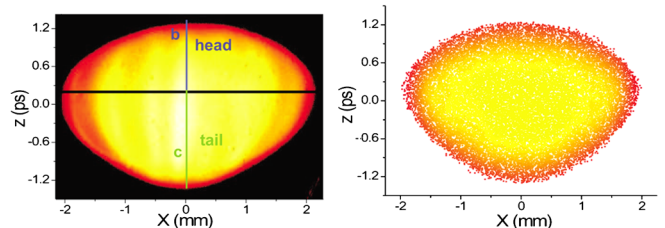


FIG. 5 (color online). Measured (left) and simulated (right) asymmetric beam distribution for $Q = 50 \text{ pC}$.

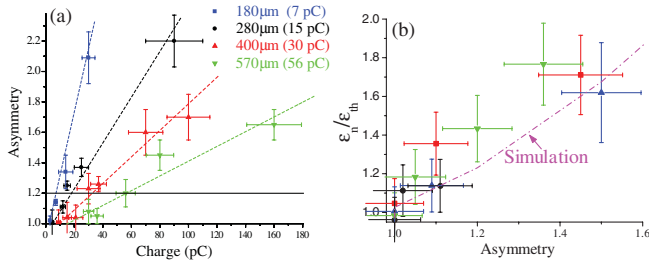


FIG. 6 (color online). (a) Measured asymmetry parameter A vs Q for different laser spot sizes at the cathode. The dashed lines are linear fits of the different sets of data. The values of beam charge for which the asymmetry parameter exceeds 1.2 are also indicated. (b) Emittance growth as a function of asymmetry parameter A .

which is $>16\%$ of the rf accelerating field at injection phase, $E_0 \sin\phi_0 \sim 34$ MV/m.

To quantify this effect, we first introduce an asymmetry parameter A defined as the ratio of the semiaxes shown in Fig. 5 (i.e., $A = b/c$). In Fig. 6 we show the dependence of A on Q and $\sigma_{L,rms}$. A linear dependence on Q is found, with a slope increasing as $\sigma_{L,rms}^{-2}$. The errors mostly come from fluctuations in the beam charge which was up to $\pm 12\%$ shot to shot due to both pulse-to-pulse laser energy jitter and pointing jitter on the laser iris aperture. In Fig. 6(b) the effect of beam asymmetry on the normalized transverse emittance ϵ_n , as measured with a multishot pepper pot technique, is illustrated. Since the beam emittance has a thermal component ϵ_{th} directly proportional to $\sigma_{L,rms}$, we normalized the measurements to the emittance values ϵ_{th} obtained for negligible (<1 pC) beam charge [14]. There is a strong correlation between A and the amount of emittance growth. When the beam loses its uniformly filled ellipsoid shape, nonlinearities associated with the space-charge fields quickly degrade the transverse quality of the beam. Values of $A > 1.2$ are to be avoided, which from the data indicate that $E_{SC,max}$ should be limited to less than 10% of the applied field $E_0 \sin\phi_0$.

The detailed experimental results presented in this Letter introduce a novel regime of rf photoinjector operation, where the beam evolution is characterized by the explosive expansion in the longitudinal dimension near the cathode—as well as non-negligible subsequent transverse expansion—under the action of the space-charge fields. The rearrangement of the beam distribution following cathode illumination by an ultrashort laser pulse well approximates a uniformly filled ellipsoid. We have further characterized a major deviation in the ellipsoidal distribution, the image charge driven asymmetry A as a function of Q , and deduced its effect on beam emittance. Operating in this regime, we obtained a 15 pC, 300 fs rms long beam with $\epsilon_n = 0.7$ mm mrad, corresponding to a peak brightness of $\sim 10^{14}$ A/m 2 , comparable with state-of-the-art photoinjectors [15]. Further improvements of the beam quality at

Pegasus can be obtained by increasing the rf gun field E_0 and reducing the thermal emittance using a different work function cathode (i.e., Cu).

Given that it produces a high quality beam, due to the linear nature of space-charge forces in ellipsoidal beams, using a less technologically demanding technique than present approaches call for, this demonstration of the blowout regime opens the door to its use in present and future electron sources. For applications where short high brightness electron beams are required at low energy, such as ultrafast relativistic electron diffraction [16], this regime may be the preferred mode of operation for rf photoinjectors. For applications that demand higher energy, such as x-ray free-electron lasers [17], a compelling next step would be to show the compatibility of the blowout regime with emittance compensation [11].

This work was supported by ONR Grant No. N000140711174 and DOE Grant No. DE-FG02-92ER40693.

-
- [1] M. Ferrario *et al.*, SLAC Report No. SLAC-PUB-8400, 2000.
 - [2] B. E. Carlsten, Nucl. Instrum. Methods Phys. Res., Sect. A **285**, 313 (1989).
 - [3] L. Serafini and J. B. Rosenzweig, Phys. Rev. E **55**, 7565 (1997).
 - [4] S. G. Anderson and J. B. Rosenzweig, Phys. Rev. ST Accel. Beams **3**, 094201 (2000).
 - [5] I. M. Kapchinskii and V. V. Vladimirskii, in *Proceedings of the 1959 International Conference on High Energy Accelerators, Geneva, Switzerland* (CERN, Geneva, 1959), p. 274.
 - [6] C. Limborg-Deprey and P. R. Bolton, Nucl. Instrum. Methods Phys. Res., Sect. A **557**, 106 (2006).
 - [7] O. J. Luiten *et al.*, Phys. Rev. Lett. **93**, 094802 (2004).
 - [8] L. Serafini, in *Towards the X-Ray Free Electron Laser*, edited by R. Bonifacio and W. A. Barletta, AIP Conf. Proc. No. 413 (AIP, New York, 1997), p. 321.
 - [9] J. B. Rosenzweig *et al.*, Int. J. Mod. Phys. A **22**, 4158 (2007).
 - [10] R. J. England *et al.*, in *Proceedings of the 2006 Advanced Accelerator Concepts Workshop*, AIP Conf. Proc. No. 877 (AIP, New York, 2006) p. 595.
 - [11] J. B. Rosenzweig *et al.*, Nucl. Instrum. Methods Phys. Res., Sect. A **557**, 87 (2006).
 - [12] K. Flottman, http://www.desy.de/?mpyflo/astra_dokumentation/.
 - [13] T. Van Oudheusden *et al.*, J. Appl. Phys. **102**, 093501 (2007).
 - [14] P. Musumeci *et al.*, in *Proceedings of the 2007 Particle Accelerator Conference, Albuquerque, NM* (IEEE, Piscataway, NJ, 2007).
 - [15] D. H. Dowell *et al.*, Phys. Rev. ST Accel. Beams **11**, 030703 (2008).
 - [16] J. Hastings *et al.*, Appl. Phys. Lett. **89**, 184109 (2006).
 - [17] <http://www-srsl.slac.stanford.edu/lcls/>.